Volatility Forecasts by Clustering: Applications for VaR Estimation

Zijin Wang
School of Economic Mathematics
Southwestern University of Finance and Economics
Chengdu, 611130, P.R. China
Tel: +86-15884554480
E-mail: 1190202Z1006@smail.swufe.edu.cn

Peimin Chen*
School of Hospitality Management
Shanghai Business School
Shanghai, 200235, P.R. China
Tel: +86-18328516475
E-mail: pmchen@sbs.edu.cn

Peng Liu
S.C. Johnson College of Business
Cornell University
Ithaca, NY, 14853, USA
Tel: 510-277-2874
Fax: 607-254-2960
E-mail: peng.liu@cornell.edu

and

Chunchi Wu*
School of Management
State University of New York
Buffalo, NY, 14260, USA
Tel: 716-645-0448
Fax: 716-645-3823
E-mail: chunchiw@buffalo.edu

*Corresponding author.

Volatility Forecasts by Clustering: Applications for VaR Estimation

Abstract

It is well known that volatility is time-varying and clustered. However, few studies have explored the information content of volatility clustering and its implications for investors' risk aversion. This information is particularly important in turbulent periods, such as financial crisis. We present a volatility cluster partition model to forecast volatility and apply it to risk management. We find that our model substantially outperforms the GARCH model and improves financial risk management using the value-at-risk metric.
Keywords: Volatility forecasts; Fisher's optimal dissection; value-at-risk.

1. Introduction

Return volatility is an important risk factor in asset pricing, portfolio selection and risk management (see Angelini et al. (2019); Schmitt and Frank (2017); Engle and Siriwardane (2018); Chen et al. (2019)). To capture instantaneous volatility dynamics and clustering, the classic Autoregressive Conditional Heteroskedasticity (ARCH) model and Generalized Autoregressive Conditional Heteroskedasticity (GARCH) model proposed by Engle (1982) and Bollerslev (1986) are popular for its simplicity and ease to interpret. Extended work, such as Nelson (1991) and Engle and Ng (1993)), examine the properties of asymmetry and high persistence. However, the GARCH-type models have some weaknesses. These models often have poor performance in describing rapid volatility changes in financial markets (see Andersen et al. (2003), Heston (2012) and Smetanina and Wu (2021)) and produce poor forecasts. On the other hand, for most financial models involving dynamic volatility (such as Heston model, CEV model, etc.), it is hard to estimate their parameters jointly using the real data, because many factors are involved and the likelihood functions are not easy to derive. For application purposes, it is desirable to have a simple volatility measure, which can incorporate current market information promptly. In this paper, we propose a volatility cluster partition model based on the clustering analysis to forecast return volatility. This model cap-

tures market information in real time and is easy to implement. Applying our model to risk management using the value-at-risk (VaR) metric, we find that it outperforms conventional methods by a substantial margin.

Stock prices can change abruptly and it is important to accommodate such a feature in volatility forecasts. As an example, since its introduction, the circuit breaker has been triggered only once on October 27, 1997, when the Dow Jones industrial index fell 7.18%, before 2020. However, from March 9 to March 18, 2020, the circuit breaker was triggered four times. Particularly, on March 16, the S&P 500 index triggered a circuit breaker at the market open for the first time in history, and the index experienced the largest one-day decline in nearly 33 years with a drop of 11.98%. Over this period, market volatility was extremely high. Ignoring the structure shift in time series can lead to inefficient volatility forecasts.

Volatility exhibits pronounced clustering. It can remain stable over a period of time but suddenly switch to another state. When volatility is in a stable mode, dynamic variations are a lesser concern and the mean of volatility is the main focus of attention. Thus, we can use the average value of volatility during a stable period as a representative volatility measure to determine the optimal time points for cluster partitions. Schmitt and Frank (2017) put forward that the herding behaviour of speculators leads to volatility clustering. When the market is calm, investors make decisions independently. But during the turbulent period, market participants are sensitive to other people's behaviour and they concentrate either on the buy or sell side. Under the unbalanced trading condition, stock prices adjust dramatically and volatility remains high.

The calm or turbulent state is usually quite persistent. However, external shocks such as financial crisis, wars or drastic changes in government policies can quickly change the regime. This can be characterized by a regime-switching (RS) process. For the RS models, a Markov process with state-dependent transition probabilities governs the switching between regimes. The maximum likelihood method is employed for the statistical inference on the optimal regime. Hamilton (1989) introduces this model to describe the U.S. business cycle, which is characterized by periodic shifts from recessions to expansions and vice versa. Klaassen (2002) proposes RS-GARCH models, in which GARCH is used in each regime to describe the volatility process. Pelletier (2006) proposes an alternative volatility model for multiple time series with the regime switching dynamic correlation.

The covariance is a constant within a regime but changes across regimes.

Signals of RS models can be phrased as structural change points, which has been traditionally detected by hypothesis tests (see, for example, Andreou and Ghysels (2002) and Lee et al. (2015)). Brown and Forsythe (1974) modify the Levene test on the equality of ex-ante and ex-post variance changes and this test is widely used in studies of stock prices (see Riordan (2012)) and futures markets (see Ederington and Lee (1993)).

Clustering analysis such as k-mean, mean-shift clustering algorithm (see Cheng (1995)), and density-based spatial clustering with noise (DBSCAN, see Ester et al. (1996)), has gained popularity in past two decades and has been developed and extended in many applied fields from statistics (see Jain (1999)) to image segmentation (see Coleman (1979)). More complicated methods, including support-vector machine and neural networks, are developed in artificial intelligence (see, for example, Zhang (2000); Shi et al. (2016)). It has been shown that these methods are efficient in dealing with the data without time order. However, in most financial models, the data involved follows a time series process and it is therefore necessary to find an alternative method to cluster the series. The Fisher's optimal dissection method is a suitable algorithm for financial modeling as it can cluster dynamic volatility by minimizing a loss function defined by the similarity of samples. The basic idea of this method is widely employed in economics (see Bai and Perron (2003)) and image treatment (see Verbesselt et al. (2010)).

In this paper, we use Fisher's optimal dissection method to model return volatility. Using this method, we identify the time points for volatility clustering and use the representative value of volatility for a stable period. For a new updated data, we can easily examine whether it belongs to the latest cluster or not. If it is, then the representative value of this cluster can be employed to predict the future volatility. If not, it is a signal of regime switch, and we need to cluster the series differently in order to produce a better volatility forecast.

Our model differs from the conventional models for structural changes in two major aspects. First, our model performs optimal volatility partitions and generates timely classification by incorporating the most updated market information. To identify the optimal classification, few observations are sufficient to implement our method. Thus, our model can capture market information much faster. This procedure contrasts with

the tests commonly used in prior research that relies on the statistical inference on the parameters of the model. In these tests, the occurrence of the structural change in parameters only reveals after enough samples are produced. As such, it cannot capture instantaneous fluctuations in volatility. To catch market information flows immediately, a more efficient method is needed. Second, the algorithm we develop is convenient and general, and there is no need to derive the inference for test statistics. It is not easy to draw an efficient statistical inference for the structural change or regime-switching model of the implied volatility calculated from the option pricing formula by the iteration method. An advantage of our algorithm is that it can incorporate the newly calculated implied volatility into the model to quickly infer the structural change.

The GARCH model has been widely used for volatility forecasts by academicians and practitioners. Orhan and Köksal (2012) compare various GARCH models for quantifying the VaR in times of stress. VaR measures the maximum likely loss of an investment portfolio within a certain time period at a confidence level. There are several main methods to estimate VaR, such as nonparametric histotical simulation and parametric variance-covariance models. In this paper, we choose GARCH as a benchmark to evaluate the performance of our model in VaR applications. We also consider other volatility models such as RSGARCH, HAR and asymmetric HAR and evaluae their performance.

This paper makes several contributions to the current literature. First, we propose a new model to cluster dynamic volatility using Fisher's optimal dissection method. A unique feature of our model is that the simulated volatility is a constant in each cluster section but can promptly respond to shocks at the cluster partition point. Second, unlike previous models, estimating the parameters of our model is relatively straightforward and the model is easy to implement. Third, our model outperforms the traditional GARCH model in volatility forecasts. Using the volatility simulated by our model, we find that it significantly improves the performance of risk management using the VaR metric. The clustering volatility estimated by our model tracks real volatility much more closely than the standard GARCH model and delivers superior forecasts for future volatilities.

The remainder of this paper is organized as follows. In Section 2, we introduce the different dynamic models of volatility. In Section 3, we present the cluster model based on Fisher's optimal dissection method. In Section 4, we discuss the applications of

our volatility measures to VaR and option price predictions and show that our method enhances the forecast of the HAR model. In Sections 5, we provide empirical results of volatility forecast and VaR. Finally, in Section 6, we summarize our main findings and conclude the paper.

2. Volatility cluster model

In this section, we provide a concise review of the classical GARCH model and recent volatility models and compare their structures.

2.1. GARCH volatility model

Assume that the time series of returns r_t, $t = 1, \ldots, T$ has the following process:

$$\begin{aligned} r_t &= \mu_t + e_t, \\ e_t &= \sigma_t \varepsilon_t, \\ \varepsilon_t &\sim D(0,1), \end{aligned} \tag{1}$$

where μ_t is the dynamic mean and e_t is residual, $\{\varepsilon_t\}$ is an independent and identically distributed innovation process with mean zero and unit variance and $\sigma_t > 0$ is the conditional volatility independent of $\{\varepsilon_t\}$. The conditional variance is measured on the past information $\mathcal{F}_{t-1}$, $\sigma_t^2 = \mathbb{E}[r_t^2|\mathcal{F}_{t-1}]$.

In the presence of volatility clustering, it is clear that σ_t is not independent but correlated to both time and previous states. The most important models measuring volatility clustering are Autoregressive Conditional Heterogeneous (ARCH) and the extended General Autoregressive Conditional Heterogeneous (GARCH) model proposed by Engle (1982) and Bollerslev (1986), respectively. A typical GARCH(p,q) can be written as

$$\sigma_t^2 = \omega + \sum_{i=1}^{q} \alpha_i r_{t-i}^2 + \sum_{j=1}^{p} \beta_j \sigma_{t-j}^2, \tag{2}$$

where ω is parameter, α_i are ARCH parameter and β_j are GARCH parameter. The conditonal variance is typically parametrized with $p = 1$ and $q = 1$ as

$$\sigma_t^2 = \omega + \alpha r_{t-1}^2 + \beta \sigma_{t-1}^2. \tag{3}$$

The standard GARCH is a convenient model that can generate a stationary process. However, it has some weaknesses. For example, it cannot model volatility asymmetry widely documented in the literature. In reality, bad news have a larger impact on volatility than good news (Conrad and Kleen (2020)), but the standard GARCH cannot not differentiate these effects. There are more elaborated recursive structures that can imposed to improve the standard GARCH model (see Glosten et al. (1993)). For the GJR-GARCH model, the conditional volatility is formulated as

$$\sigma_t^2 = \omega + \alpha r_{t-1}^2 + \gamma r_{t-1}^2 \mathbb{1}_{r_{t-1}<0} + \beta \sigma_{t-1}^2, \tag{4}$$

where $\mathbb{1}_{r_{t-1}<0}$ is an indicator function and γ is leverage parameter.

A weakness of the GARCH models is that they can not include latest volatility timely. For example, when a new return data arrives which is a drastic decrease or increase, the model will just take it into estimation with the whole data sample. This new data cannot change the parameter estimate significantly and the model cannot detect whether it is an outlier of innovation or a change of volatility.

The GARCH-type models are poorly equipped for capturing rapid changes in financial markets as pointed out by Andersen et al. (2003), Heston (2012) and Smetanina and Wu (2021), and thus give poor volatility forecasts. Especially in rapid changing periods, the forecasts are more inaccurate compared to the calm period.

2.2. Regime switching GARCH

Volatile and calm periods typically represent different regimes. Markov Regime Switch models are well suited to model different regimes. In these models, returns are dependent on state

$$r_t = \sigma_{s_t} \varepsilon_t, \tag{5}$$

where $s_t \in \{1, \ldots, N\}$ is a random variable of state at date t, satisfying a Markov process

$$P(s_t = j | s_{t-1} = i, s_{t-2}, \cdots, r_{t-1}, r_{t-2}, \cdots) = P(s_t = j | s_{t-1} = i) = p_{ij}, \tag{6}$$

where p_{ij} is the probability of switching from state i to j with $i, j \in 1, \cdots, N$.

Haas et al. (2004) proposes a regime switching GARCH (RSGARCH) model where there are N separate GARCH processes whose conditional volatility σ_{it} all exist as latent

variables at time t,

$$\sigma_{it}^2 = \omega_i + \alpha_i r_{t-1}^2 + \beta_i \sigma_{i,t-1}^2, \tag{7}$$

where parameters ω_i, α_i and β_i are dependent on state $i \in \{1, \ldots, N\}$.[1]

In practice, most applications assume only $N = 2$ or 3 different regimes though there are other models accommodating a larger number of regimes either by tightly parameterizing the relation between regimes (see Calvet and Fisher (2004)) or with prior Baysian information as Sims and Zha (2006). Estimation gets complicated with more regimes, and for simplicity and without loss of generality, we focus on the case of two regimes in the performance evaluation of different models.

2.3. HAR-RV

Realized variance (RV) is an empirical measure of daily return variability, constructed from cumulative squared intraday returns

$$RV_t^M = \sum_{i=1}^{M} r_{t,i}^2,$$

where $r_{t,i}$ is the ith logarithmic return during day t, M is the number of returns in each day. As M increases to infinity, RV is a consistent estimate of true variance (see Andersen and Bollerslev (1998), Barndorff-Nielson and Shephard (2002), Andreou and Ghysels (2009)).

Market microstructure dynamics contaminate the price process with noise, which can be time dependent and may be correlated with the efficient price (Hansen and Lunde, 2006). RV can be a biased and inconsistent estimator.[2] To reduce the effect of market microstructure noise, Liu and Maheu (2008) employ a kernel-based estimator that utilizes autocovariances of intraday returns. Specifically, Liu and Maheu (2008) follow Hansen and Lunde (2006) to provide a bias correction to realized volatility as

$$RV_t^M = \sum_{i=1}^{M} r_{t,i}^2 + 2\sum_{h=1}^{q}(1 - \frac{h}{q+1}) \sum_{i=1}^{M-h} r_{t,i} r_{t,i+h},$$

[1]For estimation, we use a MATLAB toolbox *RSGARCH* provided in Chuffart (2017).

[2]For more details on the effects of market microstructure noise on volatility estimation, please refer to Bandi and Russell (2006), Hansen and Lunde (2006), Oomen (2005), and Zhang et al. (2005).

where $q = 1$ in this calculation.

Corsi (2008) considers the heterogeneous autoregressive model (HAR) of realized volatility, which can capture many features of volatility including long memory. The logrithmic of the HAR is defined as:

$$v_t = b_0 + b_1 v_{t-1} + b_2 v_{t-5,t-1} + b_3 v_{t-22,t-1} + \varepsilon_t, \tag{8}$$

where $\varepsilon_t \sim D(0, \sigma^2)$, $v_t = \log(RV_t)$ and

$$v_{t-5,t-1} = \frac{\log(RV_{t-1}) + \log(RV_{t-2}) + \cdots + \log(RV_{t-5})}{5},$$

$$v_{t-22,t-1} = \frac{\log(RV_{t-1}) + \log(RV_{t-2}) + \cdots + \log(RV_{t-22})}{22}.$$

This model postulates three factors that affect volatility: daily log-volatility v_{t-1}, weekly moving average $v_{t-5,t-1}$, and monthly $v_{t-22,t-1}$.

To account for asymmetry and jumps, volatility can be modeled as

$$\begin{aligned} v_t =& b_0 + b_1 v_{t-1} + b_2 v_{t-5,t-1} + b_3 v_{t-22,t-1} + b_J J_{t-1} + a_1 \frac{|r_{t-1}|}{\sqrt{RV_{t-1}}} \\ &+ a_2 \frac{|r_{t-1}|}{\sqrt{RV_{t-1}}} \mathbb{1}_{r_{t-1}<0} + \epsilon_t, \end{aligned} \tag{9}$$

where J_{t-1} is a jump component defined as that in Liu and Maheu (2008)

$$J_t = \begin{cases} \log(RV_t - RBP_t + 1) & if\ RV_t - RBP_t > 0 \\ 0 & otherwise \end{cases}$$

here $RBP_t = \frac{\pi}{2} \sum_{i=1}^{M-1} |r_{t,i}||r_{t,i+1}|$ is realized bi-power variation.

Later, we compare both original HAR model and asymmetry HAR of (8) and (9).

3. Cluster partition

When there is a volatility structural change, a period of high volatility is distinguished from a period of low volatility. A key feature in our model is to use the latest structural volatility to forecast future volatility. An important task then is to detect the point of the structure change in volatility.

Given a sequence of volatility $V = (\sigma_1, \ldots, \sigma_T)$, let I be a partition point, and V is divided into two clusters if we have [3]

$$\sum_{i=1}^{T}(\sigma_i - \bar{\sigma}_i)^2 > \sum_{i_1=1}^{I-1}(\sigma_{i_1} - \bar{\sigma}_{i_1})^2 + \sum_{i_2=I}^{T}(\sigma_{i_2} - \bar{\sigma}_{i_2})^2, \tag{10}$$

where $\bar{\sigma}_i$, $\bar{\sigma}_{i_1}$ and $\bar{\sigma}_{i_2}$ are the corresponding gathering centers of $\{\sigma_i\}_{i=1}^{T}$, $\{\sigma_{i_1}\}_{i_1=1}^{I-1}$ and $\{\sigma_{i_2}\}_{i_2=I}^{T}$, respectively, $I = 2, \cdots, T$. Generally, the arithmetic or geometric mean values of the corresponding samples including the given element are used. To have an algorithm of fast speed and a simple form of model, we employ arithmetic mean values as gathering centers. The greater the difference between the left side and the right side, the more likely two different clusters. As the sum of the left side of (10) is fixed, it is equivalent to minimizing the right side. We construct the cluster statistic for a single structural change as

$$\rho_\sigma(I) = \frac{1}{T}\sum_{i_1=1}^{I-1}(\sigma_{i_1} - \bar{\sigma}_{i_1})^2 + \frac{1}{T}\sum_{i_2=I}^{T}(\sigma_{i_2} - \bar{\sigma}_{i_2})^2. \tag{11}$$

The optimal partition point can be identified as $\arg\min_{1\le i\le T}\rho_\sigma(i)$ with the minimal sum of deviation, such that the volatilities in each cluster are alike and distinctly different across clusters. This single break statistic is similar to the cumulative sum (CUSUM) test of a squared series (see Andreou and Ghysels (2002) and Xu (2013)). The difference between (11) and CUSUM is that we use conditional volatility instead. Although the squared return series is an unbiased estimator for variance, it usually contains noise. Moreover, there may be more than one partition point. We can still use basic idea of minimizing the sum of deviation among clusters to construct a statistic for multiple structural changes.

3.1. General cluster partitions of dynamic volatility

Denote a classifier $\pi : \mathbb{R}^T \mapsto \mathbb{R}^N$ as $\pi(V, N)$ and divide V into N clusters $\mathcal{C} = (C_1, \ldots, C_N)$ by N split points $(I_1, I_2, \ldots, I_N)$, where $1 = I_1 < I_2 < \cdots < I_N < T$ (define $I_{N+1} = T + 1$ for convenience). Among these clusters, the index of the first point in each cluster C_k is I_k, for $k = 1, \ldots, N$. In fact, $\pi(V, N)$ consists of N split points and

[3] In fact, we can construct a statistic inference by Chi-square test for the series $\{v_i\}_{i=1}^{T}$ to search its partition point for two clusters. But here we adopt the simple form as the inequality (10) to be consistent with the latter Fisher's optimal dissection method.

only the first point I_1 is fixed and $\pi = (I_1, I_2, \ldots, I_N) \in \mathbb{N}^+_{N-1}$.

Define a loss function of classifier π as

$$L(\pi) = \frac{1}{T} \sum_{k=1}^{N} D(V_{C_k}), \tag{12}$$

where $V_{C_k} = \{\sigma_i : i \in C_k\}$ is volatility in cluster k, $D(V_{C_k}) = \sum_{i \in C_k} d(\sigma_i, \bar{\sigma}_{C_k})$ is the diameter of cluster k with $\bar{\sigma}_{C_k}$, the central of cluster and $d(\cdot)$ is the distance function represented by the Euclidean distance.[4] The higher $D(V_{C_k})$ is, the more dispersion in cluster V_{C_k}. The loss function measures the total dispersion after classification. The optimal classifier is the one with the lowest loss function value:

$$\pi^*(V, N) = \arg \min_{\pi \in \mathbb{N}^+_{N-1}} L\left[\pi(V, N)\right]. \tag{13}$$

The optimal classifier consists of the optimal clusters $(C_1^*, \ldots, C_N^*)$. The problem of finding multiple optimal partition points in V is an essential extension of the binary classification problem in (11). Assume that the first sequential volatility has been optimally classified, then for the remaining sequence it is a binary classification problem to find a single optimal partition point. Consequently, the original optimization can be transformed into a recursive binary classification process. A forward iteration dynamic programming algorithm provides the optimal clusters and the optimal classifier $\pi^*(V, N)$ (see Appendix A for more details). In this procedure, the corresponding optimal split points are $(I_1^*, \ldots, I_N^*)$ and π^* is only dependent on conditional volatility V and cluster number N. This classifier is optimal because conditional volatility is homogeneous in each cluster and shifts apparently across clusters, which serves as a good description of volatility clustering.

For homogeneity in each cluster k, a constant $\overline{\sigma}_k$ could be a representative volatility, and cluster partition volatility $V^{CP} = (\sigma_1^{CP}, \sigma_2^{CP}, \ldots, \sigma_T^{CP})$ can be expressed as

$$\sigma_t^{CP} = \mathbb{1}_{\{t \in C_k^*\}} \overline{\sigma}_k. \tag{14}$$

[4]The distance measure can be generated by L_p-norms. The Euclidean distance is L_2-norm, taken as $d(\sigma_i, \bar{\sigma}_{C_k}) = \|\sigma_i - \bar{\sigma}_{C_k}\|_2$.

As conditional volatility $\{\sigma_t^{CP} : t \in C_k^*\}$ in each cluster are homogeneous, we set $\overline{\sigma}_k = \frac{1}{|C_k|}\sum_{i\in C_k}\sigma_i$ to be time invariant as the arithmetic average of the corresponding cluster. While there are other forms of constant representative volatility, we adopt the simplest one as above for convenience. Later we will show that different forms of average make little difference. From the homogeneous property, this partition cluster volatility of the last cluster can be applied to forecasting future volatility

$$\sigma_{T+1} = \overline{\sigma}_N.$$

In the following, we relax the constant setting to permit time dependent in each cluster and show that for the stationary time series, this representative volatility is consistent.

3.2. Cluster number

As cluster number N affects the optimal classifier, a central issue is to determine a proper cluster number. In traditional models, a natural way is to test null hypothesis that there are N clusters against the alternative of $N+1$. This test, as Hamilton (2010) argues, fails to satisfy the usual regularity conditions because under the null hypothesis, some parameters of the model would be unidentified.[5] To interpret a likelihood ratio statistic, one instead needs to appeal to the methods of Hansen (1992) or Garcia (1998). Alternative tests are not based on the likelihood ratio statistic.[6] Other alternatives are to use Bayesian methods to calculate the value of N, which implies the largest value for the marginal likelihood (see Liu and Maheu (2008)) and the Bayesian factors (see Koop and Potter (2009)), or to compare models based on their ability to forecast (see Hamilton and Susmel (1994)). However, these methods can only detect regimes usually no more than 10. In practice, the volatility evolves more dramatically, especially in crisis. Thus, we use a data-driven method to detect the cluster number.

Too many clusters may lead to over-fitting problem, which affects out-of-sample forecast performance, so we need a penalty for number of clusters.[7] We introduce an information-based statistic, which provides insight into its relationship to the optimized

[5]For example, if there is really only one cluster for the whole sample, the maximum likelihood estimation does not converge to a well-defined population magnitude, meaning that the likelihood ratio test does not have the usual χ^2 distribution.

[6]See Carrasco et al. (2014).

[7]Yao (1988) and Kühn (2001) use Schwartz Creterion to construct penalty for the number of clusters.

$L[\pi(V,N)]$ and the penalty for complexity, defined by

$$\psi(N) = \log(L[\pi(V,N)]) + \frac{N\log(T)}{T}, \tag{15}$$

where $\frac{N\log(T)}{T}$ serves as a penalty. The minimum information-based statistic leads to the optimal cluster number, which is dependent on V. We calculate the optimal cluster number before each forecasting date. This data-driven cluster number, though increasing the computation time, is much better in improving forecast accuracy than a fixed number.

3.3. Iterated cluster partition volatility

In each cluster C_k^*, a representative volatility may not be constant but a dynamic volatility which depends on the model that one is based on. These volatility models could be, but not limited to, GARCH models, Regime-Switch models and HAR, among others. Using the based model to fit volatility and to estimate parameters in each cluster, we can denote $\hat{V}_{C_k^*} = \{\hat{\sigma}_t^* : t \in C_k^*\}$ and $\hat{\theta}_k$. The volatility $\hat{V} = (\hat{V}_{C_1^*}, \ldots, \hat{V}_{C_N^*})$ is derived by N times of estimation in N clusters, with parameter $\hat{\theta}^\top = (\hat{\theta}_1^\top, \ldots, \hat{\theta}_N^\top)$. As we would expect, $\hat{V}$ reflects a stronger cluster phenomenon than V. We can also apply the cluster partition method on $\hat{V}$ to get a new classifier. Comparing this new classifier with the previous one, if they are the same, we can say that this volatility is already well clustered. If they are different, we can fit volatility again in each cluster of a new classifier. The following procedure can be iterated until a well clustered volatility is obtained, denoted as the iterated cluster partition volatility V^{ICP}.

Step 1. Fit volatility V of the whole sample.

Step 2. Apply cluster partition to V, derive an optimal classifier π_0^* and corresponding clusters $\mathcal{C}_0$.

Step 3. Fit volatility in each cluster and derive volatility $\hat{V}$.

Step 4. Apply cluster partition to $\hat{V}$, derive an optimal classifier π_1^* and corresponding clusters $\mathcal{C}_1$.

Step 5. Compare π_0^* and π_1^*. if they are the same, then $V^{ICP} = \hat{V}$. Otherwise, set $V = \hat{V}$ and repeat Step 2-5.

For every volatility model, the iterated cluster partition (ICP) method can be applied and derive a distinguished volatility. [8]

4. Comparison of models

To describe the cluster phenomenon of volatility, we first consider different volatility models before using the volatility cluster partition model. After obtaining the volatility sequence V, we then apply cluster partition and cluster partition iteration to compare the results. The models we consider are listed in Table 1.

To show the advantage of our model, we compare it with other models as we described above in both volatility forecasting and VaR estimation. In our comparative analysis, we rely on a moving-window approach. Specifically, we choose an estimation window of length $T = 750$ days (average trading days in three years). Other estimation windows of different lengths produce similar results as we show in Appendix B. We evaluate the performance of models for three adjustment frequencies l: daily ($l = 1$ day), weekly ($l = 5$ days), and monthly ($l = 22$ days). For simplicity, we only present results of 1-day ahead forecast. Readers can refer to Appendix B for the results based on other frequencies. For each forecast period t ($t = T + 1, \ldots, T + l$), the estimation window is from $t-T$ to $t-1$ using the data of previous T days to estimate the parameters required to implement a particular model. These models are then used to forecast volatility σ_t. Based on these forecast volatilities, we then calculate VaR_t. This process is iterated by adding l daily returns for the next period in the data set and dropping the corresponding earlier returns, until the end of data set is reached.

4.1. Volatility forecast

Evaluation of the volatility forecast performance is important for empirical studies that use time series because good forecasts are critical for decision making. A model is superior to another model if it provides more accurate forecasts. We use two formal loss functions, the Mean Absolute Error (MAE) and the Root Mean Squared Errors

[8] We may need a theory to prove the existence of convergence for Cluster Partition Volatility. This issue remains to be solved.

(RMSE), to evaluate the out-of-sample forecast performance of the models considered:

$$MAE = \frac{1}{n}\sum_{t=1}^{n}|\sigma_{a,t} - \sigma_{f,t}|, \tag{16}$$

$$RMSE = \sqrt{\frac{1}{n}\sum_{t=1}^{n}|\sigma_{a,t} - \sigma_{f,t}|^2} \tag{17}$$

where n is the number of forecasts, $\sigma_{a,t}$ and $\sigma_{f,t}$ refer to the true volatility and the forecast volatility associated with a particular model. Volatility is a latent variable and is unobservable. Popular proxies for volatility are unbiased measures, such as squared returns, realized volatility and range (see Patton (2011)). Among them, realized volatility is the most robust proxy and we adopt it as the proxy for true volatility. The rolling forecasting method is employed and the model with the smallest mean loss is the best one for forecasting the volatility. In addition, we use the Diebold (1995) test to pair-wisely identify the best performing model.

4.2. VaR estimation

VaR is a popular metric used in financial risk management due to its simplicity and ease of interpretation, and is widely used in investment portfolio management (Chen et al. (2019)), commodity markets (Chkili (2014)). For a given probability level α, VaR is α-quantile of the conditional distribution of the asset return. It gained a higher profile in 1994 when J.P. Morgan published its RiskMetrics system. The Basel Committee on Banking Supervision proposed in 1996 that internal VaR models may be used in the determination of the capital requirements that banks must fulfill to back their trading activities.

Let $P(r_t \leq x)$ be the probability of asset return no more than x and $F(x) = P(r_t \leq x)$ is the cumulative distribution function (CDF) of r_t. For a significance level α ($0 < \alpha < 1$), VaR is defined by

$$\mathrm{VaR}_t(\alpha) = -\sup\{x : F(x) \leq \alpha\}. \tag{18}$$

We use two main methods to estimate VaR, i.e., the historical simulation approach and the model-based mean variance method (Chen et al. (2019)). For historical simulation, returns are expected to repeat in the future. The empirical CDF of asset return

is

$$\widehat{F}^h(x) = \frac{1}{n} \sum_{\tau=t-n}^{t-1} \mathbb{1}\left(r_\tau < x\right), \tag{19}$$

where n is the window size commonly using 125, 250 and 500 trading days, corresponding to six months, one year and two years of daily observations. The forecast of VaR is

$$\widehat{\mathrm{VaR}}_t(\alpha) = -\sup\left\{x : \widehat{F}^h(x) \leq \alpha\right\}, \tag{20}$$

which is the α-quantile of the sample.

The alternative model-based mean variance approaches adopted in this paper are those based on ARMA-GARCH dynamics for conditional mean and variance as (1). VaR is calculated based on the CDF F_ε

$$\widehat{\mathrm{VaR}}_t(\alpha) = \mu_t + \sigma_t F_\varepsilon^{-1}(\alpha). \tag{21}$$

To specify the distribution of ε_t, normal and student t distributions are commonly used.

We compute VaRs at various pre-specified significance levels of α from 0.5% to 5% and evaluate these results by unconditional coverage backtest of Kupiec (1995) and the conditional coverage backtest of Engle and Ng (1993). We then examine the performance of the considered models by calculating the empirical failure rate of the return distributions. The failure rate is defined as the number of times the return series excedes the forecast VaRs. If the failure rate is equal to the pre-specified VaR level, then we can conclude that the associated VaR model is correctly specified. This hypothesis is explicitly tested by the Kupiec Likelihood Ratio (LR) test (Kupiec (1995)). The statistic of the Kupiec LR test is given by

$$LR = -2\ln\left[(1-\alpha)^{T-N}\,\alpha^N\right] + 2\ln\left[(1-f)^{T-N}\,f^N\right] \tag{22}$$

where N is the number of return observations exceeding the estimated VaR value and T is the sample size. The Kupiec LR statistic is asymptotically chi-squared distributed with one degree of freedom under the null hypothesis that the realised failure rate $f = \frac{N}{T}$ equals to the pre-specified confidence level α.

For conditional coverage backtest, we use dynamic quantile (DQ) backtest of Engle

and Ng (1993)

$$H_{t+1} - \alpha = \gamma_0 + \gamma_1 H_t(\alpha) + \gamma_2 \text{VaR}_{t+1}(\alpha) + \epsilon_{t+1}$$

estimated with least squares, $H_t = \mathbb{1}(r_\tau < \text{VaR}_t) - \alpha$. The choice of regressors refers to Berkowitz et al. (2011), and the actual backtest is then the Wald test for $\gamma_0 = \gamma_1 = \gamma_2 = 0$, which is asymptotically χ^2_3.

5. Empirical results

We consider the daily S&P 500 index, DAX 30 of German stocks and FTSE 100 index of UK stocks. Our sample period is from May 18, 2012 to May 19, 2022. Returns are measured by log returns, $r_t = \ln(P_t/P_{t-1})$ where P_t is the price at day t. In our out-of-sample forecast, we use the data from 2012 to 2016 for estimation, and reserve the remaining 6 years for evaluation and model comparison.

Table 2 presents the full-sample summary statistics of the return series. Average annualized returns range from 2.24% for FTSE to 6.63% for the S&P 500, and annualized standard deviations range from 16.48% to 20.81%. All return series exhibit mild negative skewness (around -0.6) but substantial kurtosis (13.6). The first-order auto-correlations for all these return series are close to 0, while the first-order auto-correlation of squared returns are significant positive, which shows the volatility clustering phenomenon. Statistic tests show that these series exhibit a strong ARCH effect.

Andersen et al. (2006) suggest that realized volatility is a good proxy for the true volatility. We collect 5-minite intraday indices data of S&P 500, DAX 30 and FTSE 100 from Bloomberg from 2011 to 2022 to calculate the realized volatility.

5.1. In-sample estimations of volatility models

Table 3 shows the results of standard GARCH and GJR-GARCH model estimation using the return series over the in-sample period (May 2012 to May 2016). In the first panel, we present the estimated parameters of the optimal ARMA(p,q) models, where the choice of (p,q) is made using the BIC. The R^2 values from the optimal models never rises above 1%, consistent with the well-known lack of predictability of these series. The second panel presents the parameters of the GARCH(1,1) model and the lower panel presents the estimated parameters of GJR-GARCH(1,1). The last panel presents the

parameters of RSGARCH. Parameters of HAR and HAR-a model are reported in Table 4. All of these parameters are broadly in line with the estimates in the literature.

To demonstrate the cluster partition method, we use S&P 500 for analysis in the interest of simplicity. Figure 1 shows different volatility series of S&P 500. Other results can be found in Figure 2 and 3. In Panel 1-3, we show conditional volatility estimated by GARCH, GJR-GARCH and RSGARCH. Panels 4-5 present squared returns and realized volatility. For each volatility series, we use the cluster partition method to obtain different sequences. For GARCH, we obtain 3 split points, 4 and 3 split points for GJR, RSGARCH, respectively. Only 2 split points are detected for both squared returns and relized volatility. These cluster numbers are obtained using equation (15). Among all models, clusters of GJR are more similar to squared returns and realized volatility than others. Similar results can be found also in DAX and FTSE.

To compare the in-sample performance of different models, we do in-sample volatility fitness. Based on the estimated results, we calculate fitness of volatilities campared to realized volatility. Table 5 presents the in-sample results. The upper panel shows CP and ICP improve GARCH, GJRGARCH and RSGARCH in terms of RMSE. This is common in all data. However, they do not improve MAE. RMSE is more susceptible to extreme observations than MAE, so CP and ICP perform well by absorbing error tails. The lower panel shows CP also improves both HAR and HAR-a. This improvement is significant for both MAE and RMSE.

5.2. Volatility forecast

We now turn to the out-of-sample volatility forecast perforemance. To compare the forecast performance of different models, we do out-of-sample volatility forecast with rolling window. The out-of-sample period is from May 19, 2022 to May 18, 2022 with $T = 255$. For every time point t in forecast set, we first estimate models with a fixed window size 750. For robustness, we also use window size of 500 and 1000 and the results are similar. Based on the estimated results, we forecast volatility of the next day with different models.

The volatility forecast results of different methods are reported in Table 6. Forecasts are evaluated by MAE and RMSE. In the upper panel, for S&P 500, CP and ICP improve the forecasts of GARCH, GJR and RSGARCH in both MAE and RMSE. However, they only improve GARCH and GJR for DAX and FTSE. For RSGARCH, CPRSGARCH

and ICPRSGARCH give worse forecasts. In the lower panel, we also show HAR and HAR-a forecasts. Because these two models are based on realized volatility, it is unfair to compare them with other models that require only daily returns. However, CP and ICP also improve forecast of HAR and HAR-a sometimes but not significantly.

Table 7 presents the Diebold-Mariano t-statistics on the loss differences for the S&P 500 index. Corresponding test results for other index volatility forecasts are shown in Appendix B. The tests are conducted as "row model minus column model" and so a negative number indicates that the row model outperforms the column model. The CP-GARCH and ICP-GARCH models contain all positive entries, revealing that these two models outperform other competing models. This superior performance is strongly significant for the comparisons with the GARCH, GJR, RSGARCH, CP-RSGARCH and ICP-RSGARCH. The statistics relative to CP-GJR and ICP-GJR are not significant, both below 1.96. Similar results are found for the best models for each of other index series. Notice that CP-GARCH and ICP-GARCH show no difference here, because the first calculated classifier is already stable and do not need more iteration. Similar findings are obtained for CP-GJR and ICP-GJR, whereas CP-RSGARCH and ICP-RSGARCH are different and need more iterations.

Figure 4 presents the out-of-sample volatility forecast. CP and ICP show a great performance for all three indices. To examine the robustness of our results, we also change estimation window size to 500 or 1000, and find similar results (see 10 and 11 in Appendix B).

5.3. VaR forecast

To compare the VaR forecast results from different methods, we focus on a single financial index with daily data, and the confidence levels are set at 99.5%, 99%, 97.5%, 95% 92.5% and 90%, respectively. The out-of-sample period is from 2021/05/19 to 2022/05/18 with 255 days. We also use different forecast periods, and find that all of them show similar results. The number of failure events is compared at the same confidence level to judge the merits of different models. Historical simulation is the benchmark method. From Table 8, we show Kupiec unconditional tests at the confident level of 99% and 95%. As a benchmark, historical simulation is rejected for S&P but accepted for FTSE, while for DAX it is reject at the 0.05 significance level but accepted at the 0.01 level. For other models, they are based on the normal or student-t distribution.

The performance of heavy tailed t-distribution is better than that of normal distribution, as statistics are rejected by normal distribution but accepted by t-distribution for the same model. For the student-t distribution, there are more bests, among them are GARCH, CP-GARCH, ICP-GARCH, GJR, RSGARCH, CP-RSGARCH and ICP-RSGARCH. None of these models performs best both in normal and student-t distribution. Although the HAR models give good volatility forecasts, they overestimate risk and lead to a bad VaR performances.

Moreover, we give conditional DQ tests at the confident level of 99% and 95% in Table 9. However, none of these models show significantly good results.

6. Conclusion

In this paper, we propose a volatility cluster partition model based on Fisher's optimal dissection method to forecast return volatility. Our objective is to find a model that not only can explain the volatility behavior well, but also provides a better tool for volatility forecasts. We find that our cluster partition model generates much higher accuracy in forecasting return volatility than any conventional models and offers a much more reliable tool for risk management using the VaR approach. The volatility cluster partition method may also provide more reliable volatility forecasts to better estimate option prices, which can facilitate efficient arbitrage for traders in the derivatives market and improves market efficiency. In addition, as volatility is an important factor for predicting returns (see Ang et al. (2006) and Chung et al. (2019)), better volatility forecasts by the cluster partition method facilitate asset pricing tests and investment management.

Appendix A. Forward dynamic algorithm for optimal clusters

In this appendix, we explain how we calculate the optimal cluster by a forward algorithm. For a given ordered data $V = (v_1, v_2, \cdots, v_T)$ and cluster number N, we have a classifier π with corresponding loss function $L(\pi) = \sum_{k=1}^{N} D(C_k)$, dividing V into clusters $(C_1, \ldots, C_N)$, within each cluster C_k the subscript of the first data is I_k. Denote the optimal classifier as $B(n, N) = \arg\min_\pi L[\pi(n, N)]$. By dynamic programming

principal (DPP) method, The optimal classifier satisfies

$$\begin{aligned} L(B(T,N)) &= \min L[P(T,N)] \\ &= \min_{I_N}\{L(B(I_N-1,N-1)) + D(C_N)\}, \end{aligned}$$

where I_N is the subscript of the N-th split point and the first data in the last cluster C_N. This suggests that once the last group C_N is determined, the other series $(v_1, \cdots, v_{I_N-1})$ classified into $N-1$ groups should also be optimal. This process satisfies until the classifier becomes a binary classification.

$$\begin{aligned} L(B(I_N-1,N-1)) &= \min_{I_{N-1}}\{L(B(I_{N-1}-1,N-2)) + D(C_{N-1})\}, \\ &\vdots \\ L(B(I_3-1,2)) &= \min_{I_2}\{D(C_1) + D(C_2)\}. \end{aligned}$$

Generally, a cluster includes at least several elements. Let h be the given minimum number involved in a cluster. By the recursive relations above, the algorithm searching the optimal partition points can be summarized as follows.

Step 1. Starting from $m = h+1$ to $m = n$, for each m we search the optimal partition point $I_2(m)$ of the following function by the golden section method.

$$L(B(m,2)) = \min_{I_2(m)}\{D(C_1) + D(C_2)\},$$

where $C_1(m) = \{x_{I_1}, \ldots, x_{I_2(m)-1}\}$, $C_2(m) = \{x_{I_2(m)}, \ldots, x_m\}$ and $I_1 = 1$. Further, we search the optimal position m_{opt} of m, such that the corresponding set of $\{L(B(m,2))\}_{m=h+1}^{n}$ reaches its minimum. Concurrently, we record I_3, I_2, C_1 and C_2 as $I_3 = m_{opt}$, $I_2 = I_2(m_{opt})$, $C_1 = C_1(m_{opt})$ and $C_2 = C_2(m_{opt})$, respectively.

Step 2. Suppose that we have obtained $k-1$ $(4 < k < N)$ optimal cluster partition points, $I_1, I_2, \ldots, I_{k-1}$. From the recursive relation

$$L[B(m,k)] = \min_{I_k}\{L(B(I_k-1,k-1)) + D(C_k)\},$$

the next step we need to take is to search the optimal $D(C_k)$. By the similar method to Step 1, we can obtain the optimal C_k and I_k.

Step 3. Let $k = k + 1$ for $k < N$. Repeat Step 2 until $k = N$. Then N optimal clusters are achieved.

To choose h, we use a cross validation method. Through our forecast period, $h = 80$ for DAX, and $h = 100$ for S&P 500 and FTSE.

Appendix B. Robust results for different estimation window size

In this appendix, we show robust results for different estimation window size as 500 and 1000 respectively, corresponding to 2 years and 4 years in Table 10 and Table 11.

In both Table 10 and Table 11, CP and ICP give best out-of-sample performance in the upper panel. In the lower panel, however, the advantage of CP and ICP is not significant. These results are consistent with Table 6.

We show DM test of DAX and FTSE in Table 14 and Table 15. These results are consistent with that of S&P 500 in Table 7.

References

Andersen, T.G., Bollerslev, T., (1998). Answering the skeptics: Yes, standard volatility models do provide accurate forecasts. International Economic Review, 39, 885-905.

Andersen, T.G., Bollerslev, T., Christoffersen, P.F., Diebold, F.X., (2006). Volatility and correlation forecasting. Handbook of economic forecasting, 1, 777-878.

Andersen, T.G., Bollerslev, T., Diebold, F.X., Labys, P., (2003). Modeling and forecasting realized volatility. Econometrica, 71(2), 579-625.

Andreou, E., Ghysels, E., (2002): Detecting multiple breaks in financial market volatility dynamics. Journal of Applied Econometrics, 17(5), 579-600.

Andreou, E., Ghysels, E. (2009). Structural breaks in financial time series. Handbook of financial time series, 839-870.

Ang, A., Hodrick, R.J., Xing, Y., Zhang, X., (2006): The cross-section of volatility and expected returns. Journal of Finance, 61, 259-299.

Angelini, G., Bacchiocchi, E., Caggiano, G., Fanelli, L., (2019). Uncertainty across volatility regimes. Journal of Applied Econometrics, 34(3), 437-455.

Bai, J., Perron, P., (2003). Computation and analysis of multiple structural change models. Journal of Applied Econometrics, 18(1), 1-22.

Barndorff-Nielson, O.E., Shephard, N., (2002). Estimating quadratic variation using realised variance. Journal of Applied Econometrics, 17(5), 457-477.

Berkowitz, J., Christoffersen, P., Pelletier, D. (2011). Evaluating value-at-risk models with desk-level data. Management Science, 57(12), 2213-2227.

Bollerslev, T., (1986). Generalized autoregressive conditional heteroskedasticity. Journal of Econometrics, 31(3), 307-327.

Brown, M.B., Forsythe, A.B., (1974). Robust tests for the equality of variances. Journal of the American Statistical Association, 69(346), 364-367.

Calvet, L., Fisher, A., (2004). How to forecast long-run volatility: Regime-switching and the estimation of multifractal processes. Journal of Financial Econometrics, 2, 49-83.

Campbell, J.Y., Giglio, S., Polk, C., (2018). An intertemporal CAPM with stochastic volatility. Journal of Financial Economics, 128(2), 207-233.

Carrasco, M., Hu, L. Ploberger, W., (2014). Optimal Test for Markov Switching. Econometrica, 82, 765-784.

Chen, Y., Wang, Z.C., Zhang, Z.J., (2019). Mark to market value at risk. Journal of Econometrics, 208(1), 299-321.

Cheng, Y., (1995). Mean shift, mode seeking, and clustering. IEEE Transactions on Pattern Analysis and Machine Intelligence, 17(8), 790-799.

Volatility forecasting and risk manage- ment for commodity markets in the presence of asymmetry and long memory. Energy Economics, 41, 1-18.

Chuffart, T., (2017). An implementation of markov regime switching garch models in matlab. Available at SSRN 2892688.

Chung, K. H., Wang, J., Wu, C. (2019). Volatility and the cross-section of corporate bond returns. Journal of Financial Economics, 133(2), 397-417.

Coleman, G.B., Andrews, H.C., (1979). Image segmentation by clustering. Proceedings of the IEEE, 67(5), 773-785.

Conrad, C., Kleen, O., (2020). Two are better than one: Volatility forecasting using multiplicative component garch-midas models. Journal of Applied Econometrics 35, 19-45.

Corsi, F., (2008). A simple approximate long-Memory model of realized volatility. Journal of Financial Econometrics, 7(2):174-196.

Diebold, F.X., Mariano, R.S., (1995). Comparing predictive accuracy. Journal of Business & Economic Statistics, 13, 134.

Ederington, L.H., Lee, J.H., (1993). How markets process information: news releases and volatility source. Journal of Finance, 48(4), 1161-1191.

Engle, R.F., (1982): Autoregressive conditional heteroscedasticity with estimates of the variance of United Kingdom inflation. Econometrica, 50(4), 987-999.

Engle, R.F., Ng, V.K., (1993). Measuring and testing the impact of news on volatility. Journal of Finance, 48(5), 1749-1778.

Engle, R.F., Manganelli, S., (2004). CAViaR: Conditional Autoregressive Value at Risk by Regression Quantiles. Journal of Business & Economic Statistics, 22(4), 367-381.

Engle, R.F., Siriwardane, E.N., (2018). Structural GARCH: The volatility-leverage connection. Review of Financial Studies, 31(2), 449-492.

Ester, M., Kriegel, H.P., Sander, J., Xu, X., (1996). A density-based algorithm for discovering clusters in large spatial databases with noise. Kdd, 96(34), 226-231.

Garcia, R., (1998). Asymptotic null distribution of the likelihood ratio test in markov switching models. International Economic Review, 39, 763-788.

Glosten, L.R., Jagannathan, R., Runkle, D.E., (1993). On the relation between the expected value and the volatility of the nominal excess return on stocks. Journal of Finance, 48(5), 1779-1801..

Haas, M., Mittnik, S., Paolella, M.S., (2004). A new approach to Markov-switching GARCH models. Journal of Financial Econometrics, 2(4), 493-530.

Hamilton, J.D., (1989): A new approach to the economic analysis of nonstationary time series and the business cycle. Econometrica, 2(4), 357-384.

Hamilton, J.D., Susmel, R., (1994). Autoregressive Conditional Heteroskedasticity and Changes in Regime. Journal of Econometrics, 64(1-2), 307-333.

Hamilton, J.D., (2010). Regime-Switching models. Macroeconometrics and time series analysis. Palgrave Macmillan, London, 202-209.

Hansen, B. E., (1992). The Likelihood Ratio Test under Non-Standard Conditions. Journal of Applied Econometrics, 7(S1), S61-S82.

Hansen, P.R., Huang, Z., Shek, H.H., (2012). Realized garch: a joint model for returns and realized measures of volatility. Journal of Applied Econometrics, 27(6), 877-906.

Jain, A.K., Murty, M.N., Flynn, P.J., (1999). Data clustering: a review. ACM Computing Surveys (CSUR), 31(3), 264-323.

Klaassen, F., (2002). Improving GARCH volatility forecasts with regime-switching GARCH. Empirical Economics, 27, 363-394.

Koop, G. and Potter, S. M., (2009). Prior elicitation in multiple change-point models. International Economic Review, 50(3), 751-772.

Kühn, C., (2001). An estimator of the number of change points based on weak invariance principle. Statistics & Probability Letters, 51, 189-196.

Kupiec, P.H., (1995). Techniques for verifying the accuracy of risk measurement models. Journal of Derivatives, 3(2), 73-84.

Lee, T., Kim, M., Baek, C., (2015). Tests for volatility shifts in GARCH against long-range dependence. Journal of Time Series Analysis, 36(2), 127-153.

Liu, C., Maheu, J.M., (2008). Are there structural breaks in realized volatility? Journal of Financial Econometrics, 6(3), 326-360.

Nelson, D.B., (1991): Conditional heteroskedasticity in asset returns: A new approach. Econometrica, 59(2), 347-370.

Orhan, M., Köksal, B., (2012). A comparison of GARCH models for VaR estimation. Expert Systems with Applications, 39(3), 3582-3592.

Patton, A.J., (2011). Volatility forecast comparison using imperfect volatility proxies. Journal of Econometrics, 160, 246-256.

Pelletier, D., (2006). Regime switching for dynamic correlations. Journal of Econometrics, 131(1-2), 445-473.

Riordan, R., Storkenmaier, A., (2012). Latency, liquidity and price discovery. Journal of Financial Markets, 15(4), 416-437.

Schmitt, N., Frank, W., (2017). Herding behaviour and volatility clustering in financial Markets. Quantitative Finance, 17(8), 1187-1203.

Shi, B, Bai, X, Yao, C., (2016). An end-to-end trainable neural network for image-based sequence recognition and its application to scene text recognition. IEEE Transactions on Pattern Analysis and Machine Intelligence, 39(11), 2298-2304.

Sims, C. and Zha, T., (2006). Were There Regime Switches in U.S. Monetary Policy? American Economic Review, 96(1), 54-81.

Smetanina, E., Wu, W.B., (2021). Asymptotic theory for qmle for the real-time garch(1,1) model. Journal of Time Series Analysis, 42, 752-776.

Verbesselt, J., Hyndman, R., Newnham, G., Culvenor, D., (2010). Detecting trend and seasonal changes in satellite images time series. Remote Sensing of Environment, 114(1), 106-115.

Xu, K.L., (2013). Powerful tests for structural changes in volatility. Journal of Econometrics, 173, 126-142.

Yao, Y.C., (1988). Estimating the number of change-points via Schwarz's criterion. Statistics & Probability Letters, 6, 181-189.

Zhang, G.P., Baek, C., (2019): Neural networks for classification: a survey. IEEE Transactions on Systems, Man, and Cybernetics, 30(4), 451-462.

Table 1: Model summary

Basic model	**Cluster method**	**Short**
GARCH	no clustering	GARCH
	cluster partition	CPGARCH
	iterative cluster partition	ICPGARCH
GJR-GARCH	no clustering	GJR
	cluster partition	CPGJR
	iterative cluster partition	ICPGJR
RSGARCH	no clustering	RSGARCH
	cluster partition	CPRSGARCH
	iterative cluster partition	ICPRSGARCH
HAR	no clustering	HAR
	cluster partition	CPHAR
	iterative cluster partition	ICPHAR
HAR-a	no clustering	HAR-a
	cluster partition	CPHAR-a
	iterative cluster partition	ICPHAR-a

Note: This table presents summary of models we use and the correspding short.

Table 2: Summary statistics of S&P 500, DAX, and FTSE 100

	Mean	**Std**	**Skewness**	**Kurtosis**	**Corr**(r)	**Corr**(r^2)
S&P 500	6.632	20.805	-0.555	15.701	-0.140	0.343
DAX	5.736	20.748	-0.500	10.981	0.014	0.176
FTSE 100	2.244	16.476	-0.744	13.587	-0.006	0.268

Note: This table presents summary statistics on the daily equity return series, over the full sample period from 18 May 2012 to 18 May 2022. The first two rows report the annualized mean and standard deviation of these returns in percent. Corr is the first order auto-correlation corresponding to returns and squared returns. All these three indices reflect strong ARCH effect. Codes can be found in `https://github.com/wzj5163/Cluster-partition-volatility/tree/main/Insample_estimation/Insample_estimation_1_0_1`.

Table 3: GARCH, GJR-GARCH and RS-GARCH results

	SP500	**DAX**	**FTSE**
w	0.00	0.00	0.00
α	0.17	0.09	0.12
β	0.71	0.87	0.80
w	0.00	0.00	0.00
α	0.00	0.00	0.00
β	0.76	0.85	0.80
γ	0.33	0.18	0.26
w_1	0.31	0.00	0.00
w_2	0.00	0.00	0.00
α_1	0.34	0.24	0.32
α_2	0.06	0.28	0.36
β_1	0.00	0.00	0.12
β_2	0.32	0.44	0.79
γ_1	0.32	0.16	0.79
γ_2	1.00	0.90	0.37

Note: Codes can be found in `https://github.com/wzj5163/Cluster-partition-volatility/tree/main/Insample_estimation/Insample_estimation_1_0_1`.

Table 4: HAR and HAR-a results

	SP500	**DAX**	**FTSE**
b_0	-2.78	-1.72	-1.66
b_1	0.43	0.24	0.28
b_2	0.29	0.52	0.48
b_3	0.02	0.06	0.08
b_0	-2.82	-1.68	-1.63
b_1	0.33	0.13	0.19
b_2	0.36	0.62	0.55
b_3	0.05	0.08	0.10
b_J	77.19	723.95	-1841.50
a_1	0.00	-0.06	-0.02
a_2	0.22	0.24	0.15

Note: Codes can be found in `https://github.com/wzj5163/Cluster-partition-volatility/tree/main/Insample_estimation/Insample_estimation_1_0_1`.

Table 5: Comparison of volatility in-sample fitness across competing models

	S&P 500		**DAX 30**		**FTSE 100**	
	MAE	**RMSE**	**MAE**	**RMSE**	**MAE**	**RMSE**
GARCH	0.5031	0.6228	0.8630	1.0937	0.4592	0.5744
CP-GARCH	0.5344	0.6078	0.9089	1.1169	0.4790	0.5650
ICP-GARCH	0.5332	0.6068	0.9054	1.1173	0.4805	0.5675
GJR	0.5395	0.7599	0.8445	1.1135	0.4805	0.6857
CP-GJR	0.5378	0.7268	0.8472	1.1054	0.4716	0.6638
ICP-GJR	0.5622	0.6384	0.9019	1.1065	0.4911	0.5822
RSGARCH	0.5876	0.7450	0.8775	1.1130	0.5461	0.7301
CP-RSGARCH	0.6112	0.6843	0.9185	1.1179	0.5614	0.6426
ICP-RSGARCH	0.5275	0.6177	0.8971	1.1478	0.4774	0.5993
HAR	0.2153	0.3639	0.4955	0.8389	0.2035	0.3522
CP-HAR	0.2077	0.3576	0.4804	0.8150	0.1991	0.3445
HAR-a	0.2110	0.3515	0.4835	0.8182	0.1982	0.3421
CP-HAR-a	0.2015	0.3445	0.4602	0.7838	0.1927	0.3269

Notes: This table reports the mean losses of the different volatility models over the in-sample period with respect to two valuation criteria (MAE and RMSE). Codes can be found in `https://github.com/wzj5163/Cluster-partition-volatility/tree/main/Insample_estimation/Insample_estimation_1_0_1`.

Table 6: Comparison of volatility forecasts across competing models with innovation normal-distributed and estimation window 750 days

	S&P 500		**DAX 30**		**FTSE 100**	
	MAE	**RMSE**	**MAE**	**RMSE**	**MAE**	**RMSE**
GARCH	5.76	6.85	7.01	8.44	5.59	6.42
CP-GARCH	**5.38**	**6.33**	**5.74**	7.03	5.29	**5.29**
ICP-GARCH	**5.38**	**6.33**	**5.74**	7.03	**4.56**	**5.29**
GJR	5.99	7.17	7.52	9.01	5.59	6.31
CP-GJR	5.45	6.40	6.04	**6.92**	5.15	5.85
ICP-GJR	5.45	6.40	6.05	6.98	5.15	5.85
RSGARCH	6.38	7.38	7.46	9.46	6.32	7.41
CP-RSGARCH	6.11	7.02	7.88	9.96	7.00	8.38
ICP-RSGARCH	6.04	6.96	8.41	10.52	7.00	8.43
HAR	3.26	**4.55**	3.55	4.88	2.29	3.53
CP-HAR	**3.25**	4.56	3.57	5.04	2.32	3.70
ICP-HAR	**3.25**	4.58	**3.52**	4.95	2.29	3.59
HAR-a	3.27	**4.55**	3.56	**4.82**	**2.27**	3.53
CP-HAR-a	3.32	4.64	3.59	5.08	2.28	**3.48**
ICP-HAR-a	3.31	4.64	3.54	4.92	**2.27**	3.66

Notes: This table reports the mean losses of the different volatility models over the out-of-sample period with respect to two MAE and RMSE. The values in bold face indicate best-performing models (i.e. models with the lowest mean losses). For codes, you can find in `https://github.com/wzj5163/Cluster-partition-volatility/tree/main/Volatilitypredict/Volatility_predict_1_0_1`.

Table 7: DM t-statistics on average out-of-sample loss differences, S&P 500 volatility

	GARCH	**CP-GARCH**	**ICP-GARCH**	**GJR**	**CP-GJR**	**ICP-GJR**	**RSGARCH**	**CP-RSGARCH**	**ICP-RSGARCH**
GARCH		3.91	3.91	-2.05	2.88	2.88	-4.15	-1.04	-0.64
CPGARCH	-3.91			-3.54	-0.46	-0.46	-8.31	-8.10	-7.35
ICPGARCH	-3.91			-3.54	-0.46	-0.46	-8.31	-8.10	-7.35
GJR	2.05	3.54	3.54		4.86	4.86	-0.95	0.60	0.85
CPGJR	-2.88	0.46	0.46	-4.86			-5.84	-3.85	-3.44
ICPGJR	-2.88	0.46	0.46	-4.86			-5.84	-3.85	-3.44
RSGARCH	4.15	8.31	8.31	0.95	5.84	5.84		3.80	4.53
CPRSGARCH	1.04	8.10	8.10	-0.60	3.85	3.85	-3.80		1.39
ICPRSGARCH	0.64	7.35	7.35	-0.85	3.44	3.44	-4.53	-1.39	

Notes: This table present t-statistics from Diebold-Mariano tests comparing the average loss, over the out-of-sample period from May 2021 to May 2022 for different forecast models. A positive value indicates that the column model has lower average loss difference than the row model. Value greater than 1.96 in absolute value indicate that the average loss difference is significantly different from zero at the 95% confidence level. For codes, you can find in `https://github.com/wzj5163/Cluster-partition-volatility/tree/main/Volatility_predict/Volatility_predict_2020220907`.

Table 8: Kupiec unconditional tests of S&P 500

	$\alpha = 0.01$			$\alpha = 0.05$		
	S&P 500	**DAX**	**FTSE**	**S&P 500**	**DAX**	**FTSE**
Historical Simulation	0.0015	**0.1775**	**0.3956**	0.0283	0.0169	**0.3603**
GARCH-N	*0.0635*	0.0220	**0.1707**	**0.1499**	*0.0992*	**0.9314**
GARCH-t	**0.7236**	**0.7828**	**0.3956**	**0.3603**	*0.0992*	**0.9314**
CP-GARCH-N	*0.0635*	0.0064	0.0060	*0.0900*	**0.1634**	**0.5192**
CP-GARCH-t	**0.7779**	**0.4071**	**0.1707**	**0.1499**	**0.1634**	**0.5192**
ICP-GARCH-N	*0.0635*	0.0064	0.0060	*0.0900*	**0.1634**	**0.5192**
ICP-GARCH-t	**0.7236**	**0.4071**	**0.1707**	**0.1499**	**0.1634**	**0.5192**
GJR-N	*0.0635*	0.0220	**0.1707**	**0.2381**	**0.1634**	**0.7125**
GJR-t	**0.7236**	**0.7100**	**0.3956**	**0.3603**	**0.1634**	**0.8389**
CP-GJR-N	0.0207	0.0064	0.0207	*0.0900*	**0.1634**	**0.7125**
CP-GJR-t	**0.3956**	**0.7928**	**0.3956**	*0.0900*	**0.1634**	**0.7125**
ICP-GJR-N	0.0207	0.0064	0.0207	*0.0900*	**0.1634**	**0.7125**
ICP-GJR-t	**0.3956**	**0.7928**	**0.3956**	*0.0900*	**0.1634**	**0.7125**
RSGARCH-N	**0.1707**	**0.4071**	*0.0635*	**0.1499**	**0.5484**	**0.8389**
RSGARCH-t	**0.2684**	**0.4071**	**0.3956**	**0.3603**	**0.5484**	**0.4202**
CP-RSGARCH-N	*0.0635*	**0.1775**	*0.0635*	*0.0900*	**0.5484**	**0.4202**
CP-RSGARCH-t	**0.2684**	**0.7928**	**0.3957**	**0.1499**	**0.5484**	**0.4202**
ICP-RSGARCH-N	*0.0635*	**0.4071**	*0.0635*	**0.2381**	**0.9658**	**0.4202**
ICP-RSGARCH-t	**0.2684**	**0.4071**	**0.7779**	**0.2381**	**0.9658**	**0.4202**
HAR-N	0.0000	0.0000	0.0000	0.0000	0.0000	0.0001
HAR-t	0.0000	0.0001	0.0015	0.0000	0.0000	0.0003
CP-HAR-N	0.0000	0.0000	0.0000	0.0000	0.0000	0.0001
CP-HAR-t	0.0000	0.0000	0.0004	0.0000	0.0000	0.0001
ICP-HAR-N	0.0000	0.0000	0.0000	0.0000	0.0000	0.0001
ICP-HAR-t	0.0000	0.0000	0.0015	0.0000	0.0000	0.0001
HAR-a-N	0.0000	0.0000	0.0000	0.0000	0.0000	0.0001
HAR-a-t	0.0000	0.0001	0.0015	0.0000	0.0000	0.0003
CP-HAR-a-N	0.0000	0.0000	0.0000	0.0000	0.0000	0.0001
CP-HAR-a-t	0.0000	0.0000	0.0004	0.0000	0.0000	0.0001
ICP-HAR-a-N	0.0000	0.0000	0.0000	0.0000	0.0000	0.0001
ICP-HAR-a-t	0.0000	0.0000	0.0004	0.0000	0.0000	0.0001

Notes: This table presents p-values from the Kupiec unconditional tests of VaR. Values that are greater than 0.1 (indicating no evidence against the corresponding level) are in bold, and values between 0.05 and 0.1 are in italics. Codes can be found in `https://github.com/wzj5163/Cluster-partition-volatility/tree/main/VaR_predict_and_test/VaR_predict_and_test_20220913`.

Table 9: DQ tests

	$\alpha = 0.01$			$\alpha = 0.05$		
	S&P 500	**DAX**	**FTSE**	**S&P 500**	**DAX**	**FTSE**
Historical Simulation	0.0000	0.0016	0.0055	**0.6141**	**0.2573**	0.0476
GARCH-N	0.0000	0.0005	0.0250	0.0000	**0.1746**	**0.6678**
GARCH-t	0.0000	0.0000	*0.0783*	0.0000	**0.1746**	**0.6678**
CP-GARCH-N	0.0000	0.0021	**0.1578**	0.0000	**0.3725**	**0.2740**
CP-GARCH-t	0.0000	0.0000	0.0000	0.0000	**0.3725**	**0.2740**
ICP-GARCH-N	0.0000	0.0021	**0.1578**	0.0000	**0.3725**	**0.2740**
ICP-GARCH-t	0.0000	0.0000	0.0000	0.0000	**0.3725**	**0.2740**
GJR-N	0.0000	0.0003	0.0313	0.0000	**0.1503**	**0.3941**
GJR-t	0.0000	0.0000	**0.1274**	0.0000	**0.1503**	**0.9009**
CP-GJR-N	0.0000	0.0000	0.0000	0.0000	**0.5317**	**0.2313**
CP-GJR-t	0.0000	0.0000	0.0033	0.0000	**0.5317**	**0.2313**
ICP-GJR-N	0.0000	0.0000	0.0000	0.0000	**0.5304**	**0.2313**
ICP-GJR-t	0.0000	0.0000	0.0033	0.0000	**0.5304**	**0.2313**
RSGARCH-N	0.0000	0.0232	0.0201	0.0000	**0.5816**	**0.4637**
RSGARCH-t	0.0000	0.0232	0.0409	0.0000	**0.5816**	0.0000
CP-RSGARCH-N	0.0000	0.0001	0.0026	0.0001	**0.4407**	0.0018
CP-RSGARCH-t	0.0000	0.0000	0.0197	0.0000	**0.4407**	0.0018
ICP-RSGARCH-N	0.0000	*0.0588*	0.0280	0.0242	**0.6156**	0.0006
ICP-RSGARCH-t	**1.0000**	*0.0588*	0.0146	0.0242	**0.6156**	0.0006
HAR-N	0.0001	0.0001	0.0002	0.0000	0.0018	0.0026
HAR-t	0.0275	0.0055	0.0000	0.0000	0.0018	0.0031
CP-HAR-N	0.0000	0.0009	0.0003	0.0000	0.0014	0.0024
CP-HAR-t	0.0098	0.0039	0.0152	0.0001	0.0014	0.0024
ICP-HAR-N	0.0000	0.0003	0.0003	0.0000	0.0007	0.0016
ICP-HAR-t	0.0326	0.0032	0.0000	0.0001	0.0007	0.0030
HAR-a-N	0.0001	0.0004	0.0003	0.0001	0.0063	0.0029
HAR-a-t	0.0000	0.0060	0.0000	0.0001	0.0063	0.0035
CP-HAR-a-N	0.0001	0.0053	0.0003	0.0000	0.0061	0.0032
CP-HAR-a-t	0.0000	0.0047	0.0000	0.0000	0.0061	0.0032
ICP-HAR-a-N	0.0000	0.0002	0.0002	0.0000	0.0039	0.0018
ICP-HAR-a-t	0.0001	0.0041	0.0000	0.0000	0.0039	0.0018

Notes: This table reports the mean losses of the different volatility models over the in-sample period with respect to two valuation criteria (MAE and RMSE). Codes can be found in `https://github.com/wzj5163/Cluster-partition-volatility/tree/main/VaR_predict_and_test/VaR_predict_and_test_20220913`.

Table 10: Comparison of volatility forecasts across competing models with innovation normal-distributed and estimation window 500 days

	S&P 500		**DAX 30**		**FTSE 100**	
	MAE	**RMSE**	**MAE**	**RMSE**	**MAE**	**RMSE**
GARCH	5.76	6.85	7.01	8.44	5.59	6.42
CP-GARCH	**5.60**	6.63	**6.51**	**8.01**	**4.62**	**5.26**
ICP-GARCH	5.61	6.63	6.78	8.24	4.68	5.32
GJR	5.99	7.17	7.52	9.01	5.59	6.31
CP-GJR	5.65	**6.57**	6.91	8.53	4.84	5.44
ICP-GJR	5.66	**6.57**	6.88	8.60	4.72	5.34
RSGARCH	6.38	7.38	7.46	9.46	6.32	7.41
CP-RSGARCH	16.63	88.43	9.37	11.69	7.69	9.04
ICP-RSGARCH	11.71	45.65	9.66	11.93	7.58	8.94
HAR	3.26	**6.99**	3.55	4.88	2.29	3.20
CP-HAR	**3.24**	7.20	**3.53**	5.01	2.29	3.21
ICP-HAR	**3.24**	7.21	**3.53**	5.00	2.28	3.17
HAR-a	3.27	7.07	3.56	**4.82**	**2.27**	3.14
CP-HAR-a	3.33	7.26	3.57	4.95	2.28	3.14
ICP-HAR-a	3.35	7.26	3.58	4.93	**2.27**	**3.12**

Notes: This table reports the mean losses of the different volatility models over the out-of-sample period with respect to two MAE and RMSE. The values in bold face indicate best-performing models (i.e. models with the lowest mean losses). For codes, you can find in `https://github.com/wzj5163/Cluster-partition-volatility/tree/main/Volatilitypredict/Volatility_predict_1_0_3`.

Table 11: Comparison of volatility forecasts across competing models with innovation normal-distributed and estimation window 1000 days

	S&P 500		**DAX 30**		**FTSE 100**	
	MAE	**RMSE**	**MAE**	**RMSE**	**MAE**	**RMSE**
GARCH	5.76	6.85	7.01	8.44	5.59	6.42
CP-GARCH	**5.38**	**6.33**	**5.92**	7.56	**4.53**	**5.24**
ICP-GARCH	**5.38**	**6.33**	**5.92**	7.56	**4.53**	**5.24**
GJR	5.99	7.17	7.52	9.01	5.59	6.31
CP-GJR	5.45	6.40	6.06	**6.99**	5.16	5.85
ICP-GJR	5.45	6.40	6.10	7.05	5.16	5.85
RSGARCH	6.38	7.38	7.46	9.46	6.32	7.41
CP-RSGARCH	5.88	6.97	6.53	8.17	6.53	8.08
ICP-RSGARCH	5.84	6.88	6.87	8.36	6.50	7.97
HAR	3.26.	**4.55**	3.55	4.88	2.29	3.20
CP-HAR	3.25	4.56	3.57	5.11	2.30	3.26
ICP-HAR	**3.24**	4.57	3.56	5.04	2.31	3.26
HAR-a	3.27.	**4.55**	3.56	**4.82**	2.27	**3.14**
CP-HAR-a	3.33	4.64	**3.51**	4.92	**2.26**	3.18
ICP-HAR-a	3.31	4.63	3.52	4.90	**2.26**	3.16

Notes: This table reports the mean losses of the different volatility models over the out-of-sample period with respect to two MAE and RMSE. The values in bold face indicate best-performing models (i.e. models with the lowest mean losses). For codes, you can find in `https://github.com/wzj5163/Cluster-partition-volatility/tree/main/Volatilitypredict/Volatility_predict_1_0_4`.

Table 12: Comparison of volatility forecasts across competing models with innovation normal-distributed and estimation window 1000 days

	S&P 500		**DAX 30**		**FTSE 100**	
	MAE	**RMSE**	**MAE**	**RMSE**	**MAE**	**RMSE**
GARCH	5.76	6.85	7.01	8.44	5.60	6.42
CP-GARCH	**5.38**	**6.33**	5.92	7.56	**4.53**	**5.24**
ICP-GARCH	**5.38**	**6.33**	5.92	7.56	**4.53**	**5.24**
GJR	5.99	7.17	7.52	9.02	5.59	7.35
CP-GJR	5.45	8.87	**6.06**	**6.99**	5.16	5.85
ICP-GJR	5.45	6.40	6.10	7.05	5.16	5.85
RSGARCH	6.38	6.40	7.46	9.46	6.32	7.41
CP-RSGARCH	5.88	5.88	6.53	8.17	6.53	8.08
ICP-RSGARCH	5.84	5.58	6.87	8.36	6.50	7.97
HAR	3.26	**4.55**	3.55	4.88	2.29	3.20
CP-HAR	3.25	4.56	3.57	5.11	2.30	3.26
ICP-HAR	**3.24**	4.57	3.56	5.04	2.31	3.26
HAR-a	3.27	**4.55**	3.56	**4.82**	2.27	**3.14**
CP-HAR-a	3.33	4.64	**3.51**	4.92	**2.26**	3.18
ICP-HAR-a	3.31	4.63	3.52	4.90	**2.26**	3.16

Notes: This table reports the mean losses of the different volatility models over the out-of-sample period with respect to two MAE and RMSE. The values in bold face indicate best-performing models (i.e. models with the lowest mean losses). For codes, you can find in `https://github.com/wzj5163/Cluster-partition-volatility/tree/main/Volatility%20predict/Volatility_predict_1_0_4`.

Table 13: Comparison of volatility forecasts across competing models with innovation normal-distributed and estimation window 500 days

	S&P 500		**DAX 30**		**FTSE 100**	
	MAE	**RMSE**	**MAE**	**RMSE**	**MAE**	**RMSE**
GARCH	5.76	6.85	7.01	8.44	5.60	6.42
CP-GARCH	**5.38**	**6.33**	5.92	7.56	**4.53**	**5.24**
ICP-GARCH	**5.38**	**6.33**	5.92	7.56	**4.53**	**5.24**
GJR	5.99	7.17	7.52	9.02	5.59	7.35
CP-GJR	5.45	8.87	**6.06**	**6.99**	5.16	5.85
ICP-GJR	5.45	6.40	6.10	7.05	5.16	5.85
RSGARCH	6.38	6.40	7.46	9.46	6.32	7.41
CP-RSGARCH	5.88	5.88	6.53	8.17	6.53	8.08
ICP-RSGARCH	5.84	5.58	6.87	8.36	6.50	7.97
HAR	3.26	**4.55**	3.55	4.88	2.29	3.20
CP-HAR	3.25	4.56	3.57	5.11	2.30	3.26
ICP-HAR	**3.24**	4.57	3.56	5.04	2.31	3.26
HAR-a	3.27	**4.55**	3.56	**4.82**	2.27	**3.14**
CP-HAR-a	3.33	4.64	**3.51**	4.92	**2.26**	3.18
ICP-HAR-a	3.31	4.63	3.52	4.90	**2.26**	3.16

Notes: This table reports the mean losses of the different volatility models over the out-of-sample period with respect to two MAE and RMSE. The values in bold face indicate best-performing models (i.e. models with the lowest mean losses). For codes, you can find in `https://github.com/wzj5163/Cluster-partition-volatility/tree/main/Volatility%20predict/Volatility_predict_1_0_4`.

Table 14: DM t-statistics on average out-of-sample loss differences, DAX 30 volatility

	GARCH	**CP-GARCH**	**ICP-GARCH**	**GJR**	**CP-GJR**	**ICP-GJR**	**RSGARCH**	**CP-RSGARCH**	**ICP-RSGARCH**
GARCH		6.49	6.49	-1.49	3.95	3.95	-2.52	-3.14	-4.12
CPGARCH	-6.49			-4.17	0.31	0.17	-4.82	-5.24	-6.17
CPGARCH	-6.49			-4.17	0.31	0.17	-4.82	-5.24	-6.17
GJR	1.49	4.17	4.17		4.99	4.90	-0.83	-1.56	-2.45
CPGJR	-3.95	-0.31	-0.31	-4.99		-1.13	-4.14	-4.45	-5.33
ICPGJR	-3.95	-0.17	-0.17	-4.90	1.13		-4.09	-4.40	-5.28
RSGARCH	2.52	4.82	4.82	0.83	4.14	4.08		-1.97	-3.66
CPRSGARCH	3.14	5.24	5.24	1.56	4.45	4.40	1.97		-2.03
ICPRSGARCH	4.12	6.17	6.17	2.45	5.33	5.28	3.66	2.03	

Notes: This table present t-statistics from Diebold-Mariano tests comparing the average loss, over the out-of-sample period from May 2021 to May 2022 for different forecast models. A positive value indicates that the column model has lower average loss difference than the row model. Value greater than 1.96 in absolute value indicate that the average loss difference is significantly different from zero at the 95% confidence level. For codes, you can find in `https://github.com/wzj5163/Cluster-partition-volatility/tree/main/Volatilitypredict/Volatility_predict_1_0_1`.

Table 15: DM t-statistics on average out-of-sample loss differences, FTSE 100 volatility

	GARCH	**CP-GARCH**	**ICP-GARCH**	**GJR**	**CP-GJR**	**ICP-GJR**	**RSGARCH**	**CP-RSGARCH**	**ICP-RSGARCH**
GARCH		5.86	5.86	1.28	3.50	3.50	-4.57	-4.29	-4.34
CPGARCH	-5.86			-6.06	-7.66	-7.66	-6.44	-5.77	-5.74
ICPGARCH	-5.86			-6.06	-7.66	-7.66	-6.44	-5.77	-5.74
GJR	-1.28	6.06	6.06		3.35	3.35	-4.49	-4.41	-4.49
CPGJR	-3.50	7.66	7.66	-3.35			-5.05	-4.86	-4.88
ICPGJR	-3.50	7.66	7.66	-3.35			-5.05	-4.86	-4.88
RSGARCH	4.57	6.44	6.44	4.49	5.05	5.05		-3.10	-3.36
CPRSGARCH	4.29	5.77	5.77	4.41	4.86	4.86	3.10		-0.51
ICPRSGARCH	4.34	5.74	5.74	4.49	4.88	4.88	3.34	0.51	

Notes: This table present t-statistics from Diebold-Mariano tests comparing the average loss, over the out-of-sample period from May 2021 to May 2022 for different forecast models. A positive value indicates that the column model has lower average loss difference than the row model. Value greater than 1.96 in absolute value indicate that the average loss difference is significantly different from zero at the 95% confidence level. For codes, you can find in `https://github.com/wzj5163/Cluster-partition-volatility/tree/main/Volatilitypredict/Volatility_predict_1_0_1`.

Figure 1: Cluster Partition Volatility of S&P 500 index. In Panel 1-3, we show conditional volatility estimated by GARCH, GJR-GARCH and RSGARCH. Panel 4-5 present squared returns and realised volatility. For each volatility series, we use cluster partition method to get different sequences. Codes can be found in `https://github.com/wzj5163/Cluster-partition-volatility/tree/main/Insample_estimation/Insample_estimation_20220905`.

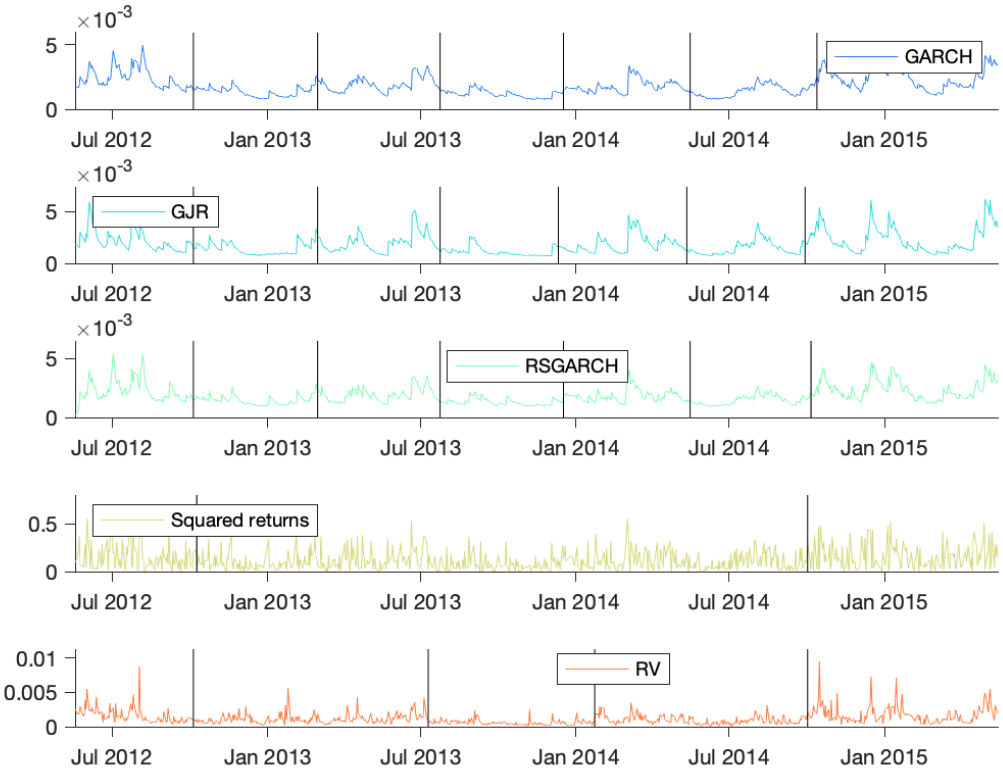

Figure 2: Cluster Partition Volatility of dx 30 index. In Panel 1-3, we show conditional volatility estimated by GARCH, GJR-GARCH and RSGARCH. Panel 4-5 present squared returns and realised volatility. For each volatility series, we use cluster partition method to get different sequences. Codes can be found in `https://github.com/wzj5163/Cluster-partition-volatility/tree/main/Insample_estimation/Insample_estimation_20220905`.

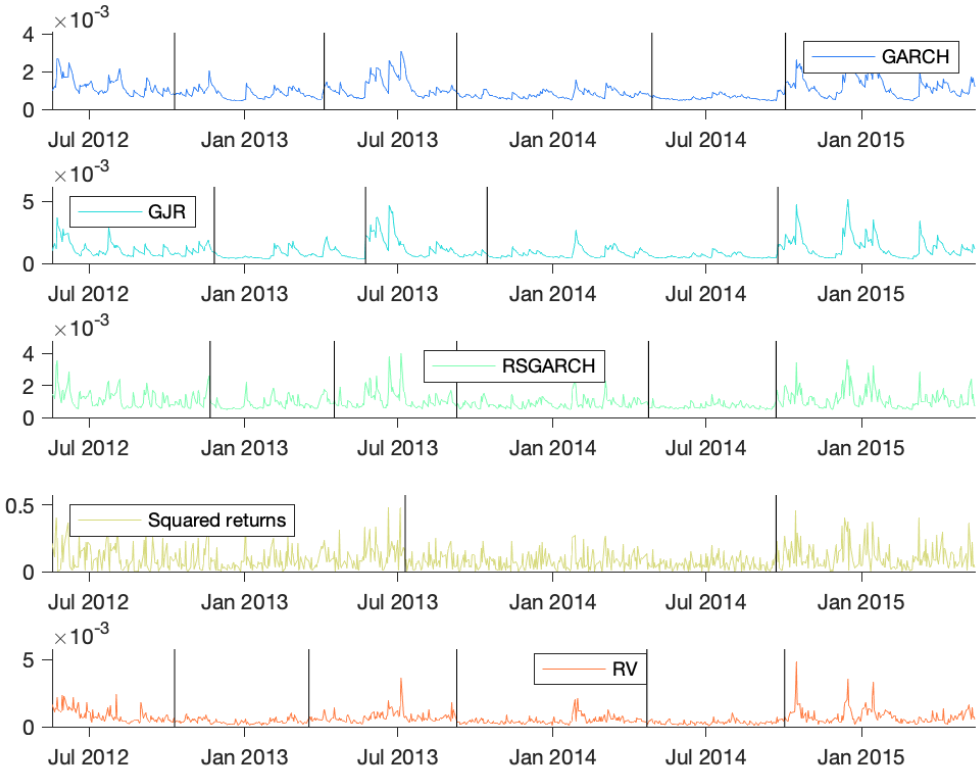

Figure 3: Cluster Partition Volatility of FTSE 100 index. In Panel 1-3, we show conditional volatility estimated by GARCH, GJR-GARCH and RSGARCH. Panel 4-5 present squared returns and realised volatility. For each volatility series, we use cluster partition method to get different sequences. Codes can be found in `https://github.com/wzj5163/Cluster-partition-volatility/tree/main/Insample_estimation/Insample_estimation_20220905`.

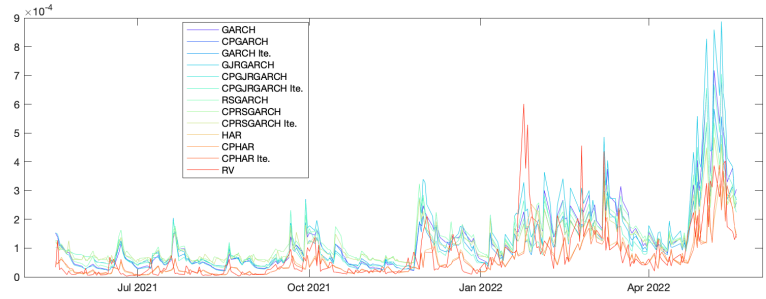

Panel A. S&P 500 index

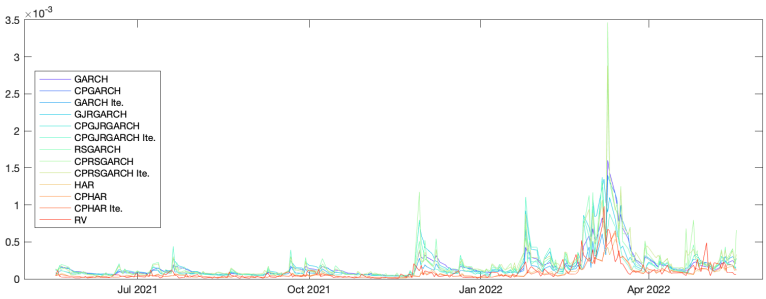

Panel B. DAX 30 index

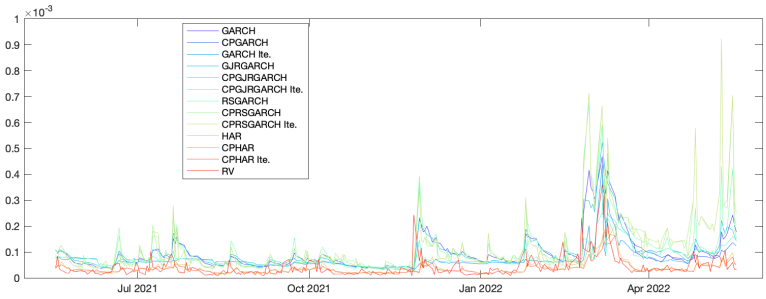

Panel C. FTSE 100 index

Figure 4: Volatility forecast

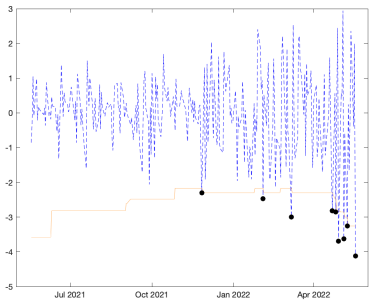

Figure 5: Historical simulation

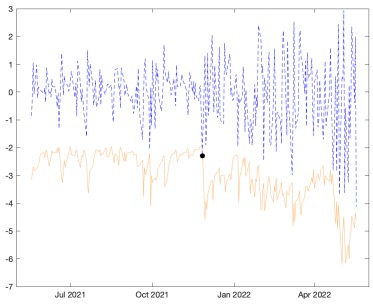

Figure 6: CP-RSGARCH-t with $\alpha = 0.01$